

Monte Carlo Calculations of Acoustic Wave Propagation in the Turbulent Atmosphere*

Vladimir Belov, Yulia Burkatovskaya, Nikolay Krasnenko, and Luidmila Shamanaeva

Institute of Atmospheric Optics SB RAS,
1, Akademicheskii Ave., Tomsk 634055, Russia
Institute of Cybernetics, National Research Tomsk Polytechnical University,
30 Lenin Prospekt, 634050 Tomsk, Russia
Department of Applied Mathematics and Cybernetics,
National Research Tomsk State University,
36 Lenin Prospekt, 634050 Tomsk, Russia
Institute of Monitoring of Climatic and Ecological Systems SB RAS
10/3, Akademicheskii Ave., Tomsk 634055, Russia
Tomsk State University of Control Systems and Radioelectronics
40 Lenin Prospekt, 634050 Tomsk, Russia
{belov,sima}@iao.ru, tracey@tpu.ru, krasnenko@imces.ru

Abstract. The problem of acoustic wave propagation in the turbulent atmosphere is solved by the Monte Carlo method. A 500-m plane-stratified model of the turbulent atmosphere is considered. Classical and molecular absorption of acoustic radiation and scattering by turbulent temperature and wind velocity fluctuations are taken into account for acoustic radiation frequencies of 1, 2, 3 and 4 kHz. A good agreement of the simulation results with experimentally measured values demonstrates the efficiency of the suggested algorithm.

Keywords: atmosphere, turbulence, acoustic wave propagation, Monte-Carlo calculations.

1 Introduction

Investigations of sound propagation in the atmosphere are necessary for the prediction of its characteristics, finding direction toward a sound source, and quantitative interpretation of the data of acoustic sounding [1]. In the outdoor atmosphere, the sound propagation is influenced by a large number of factors, including the vertical atmospheric stratification, turbulence, viscosity, and effects caused by finite dimensions of sound beams in the transverse direction, that is, by the angular divergence of acoustic beams broadened due to the atmospheric

* This work was supported in part by the Scientific Research executed within the framework of the Special Federal Program "Scientific and Pedagogical Personnel of Innovative Russia" for 2009-2013 (Contracts Nos. 02.740.11.0232 and 14.740.11.0204).

turbulence [2, 3]. Difficulties of analytical approaches to a solution of the problem of acoustic radiation transfer through the outdoor atmosphere call for the use of numerical methods (for example, see [4, 5]), from which the method of statistical simulation (Monte Carlo) is most promising [6, 7]. This method allows sound scattering on the acoustic refractive index fluctuations caused by wind velocity and temperature inhomogeneities to be taken into account for the most realistic models of the atmosphere.

The equation of acoustic radiation transfer in the turbulent atmosphere in the form of the Neumann series for the acoustic ray intensity was derived in [8]. In [9], the Monte Carlo method was first used to solve the problem of acoustic wave propagation through a vertically stratified turbulent atmosphere. The density of collisions of acoustic particles - phonons - was estimated in terms of the acoustic energy flux density scattered by the atmospheric turbulence derived in [10] in the single scattering approximation.

In the present work, we use the modified Monte Carlo algorithm to solve the problem of acoustic radiation propagation in the atmosphere.

2 Model of the Atmosphere and Geometry of the Numerical Experiment

For a 500-m standard plane-stratified turbulent atmosphere, the total attenuation coefficient was calculated from the formula

$$\sigma_{att}(z_i) = \sigma_{cl} + \sigma_{mol}(z_i) + \sigma_T(z_i) + \sigma_V(z_i), \quad (1)$$

where σ_{cl} and $\sigma_{mol}(z_i)$ are the coefficients of classical and molecular absorption, $\sigma_T(z_i)$ and $\sigma_V(z_i)$ are the coefficients of scattering by turbulent temperature and wind velocity fluctuations, $z_i = z_{i-1} + dz$, $dz = 20\text{m}$, $i = 1, \dots, 26$, and $z_0 = 0$.

The coefficients of classical and molecular absorption σ_{cl} and $\sigma_{mol}(z_i)$, in m^{-1} , were taken from [11, 12].

Analytical expressions for the scattering coefficients were derived in [9, 13] for the von Karman model of the three-dimensional spectra of temperature and wind velocity fluctuations:

$$\begin{aligned} \sigma_T(z_i) = & 0.9\lambda^{-1/3}(z_i)C_T^2(z_i)T^{-2}(z_i)L_0^{-7/3}(z_i) \\ & \times \left\{ 0.07143 [B^{7/6}(z_i) - \lambda^{7/3}(z_i)] - 0.1A^2(z_i) [B^{-5/6}(z_i) - \lambda^{-5/3}(z_i)] \right. \\ & \left. - A(z_i) [B^{1/6}(z_i) - \lambda^{1/3}(z_i)] \right\}; \end{aligned} \quad (2)$$

$$\begin{aligned} \sigma_V(z_i) = & 1.569\varepsilon^{2/3}(z_i)\lambda^{-1/3}(z_i)c^{-2}(z_i)L_0^{-13/3}(z_i) \\ & \times \left\{ 0.1429 [B(z_i) + 2A(z_i)] [B^{7/6}(z_i) - \lambda^{7/3}(z_i)] \right. \\ & - 0.0769 [B^{13/6}(z_i) - \lambda^{13/3}(z_i)] - A(z_i) [A(z_i) + 2B(z_i)] \\ & \left. \times [B^{1/6}(z_i) - \lambda^{1/3}(z_i)] - 0.2A^2(z_i)B(z_i) [B^{-5/6}(z_i) - \lambda^{-5/3}(z_i)] \right\}, \end{aligned} \quad (3)$$

where $\lambda(z_i)$ is the wavelength, $c(z_i)$ is the velocity of sound, $L_0(z_i)$ in the outer scale of the atmospheric turbulence, $C_T^2(z_i)$ is the structure function of the wind velocity field $T(z_i)$, $\varepsilon(z_i)$ is the kinetic energy dissipation rate,

$$\begin{aligned} A(z_i) &= 2L_0^2(z_i) + \lambda^2(z_i); \\ B(z_i) &= 4L_0^2 + \lambda^2(z_i). \end{aligned} \quad (4)$$

The normalized scattering phase functions were calculated from the following formulas [9, 13]

$$\begin{aligned} g_T(z_i, \theta) &= 0.1062L_0^6(z_i) \cos^2 \theta [2L_0^2(z_i)(1 - \cos \theta) + \lambda^2(z_i)]^{-11/6} \\ &\times \left\{ 0.07143 [B^{7/6}(z_i) - \lambda^{7/3}(z_i)] - 0.1A^2(z_i) [B^{-5/6}(z_i) - \lambda^{-5/3}(z_i)] \right. \\ &\quad \left. - A(z_i) [B^{1/6}(z_i) - \lambda^{1/3}(z_i)] \right\}^{-1}; \end{aligned} \quad (5)$$

$$\begin{aligned} g_V(z_i, \theta) &= 0.1191L_0^{13/3}(z_i) \cos^2 \theta (1 + \cos \theta) \left(\frac{A(z_i)}{2L_0^2(z_i)} - \cos \theta \right)^{-11/6} \\ &\times \left\{ 0.1429 [B(z_i) + 2A(z_i)] [B^{7/6}(z_i) - \lambda^{7/3}(z_i)] \right. \\ &\quad \left. - 0.0763 [B^{13/6}(z_i) - \lambda^{13/3}(z_i)] - A(z_i) [A(z_i) + 2B(z_i)] \right. \\ &\quad \left. \times [B^{1/6}(z_i) - \lambda^{1/3}(z_i)] - 0.2A^2(z_i)B(z_i) [B^{-5/6}(z_i) - \lambda^{-5/3}(z_i)] \right\}^{-1}. \end{aligned} \quad (6)$$

Calculations were performed for point-sized and finite-aperture (circular aperture with a diameter of 1m.) sound sources with acoustic power of 1W placed at altitude z_s above the Earth's surface for frequencies of 1, 2, 3, and 4kHz typically used in sodars (acoustic radars) [1]. Emitted radiation was continuous in the solid angle subtended by the circular cone of half-angle $\phi = 2.5, 5, 10, 15, 20,$ and 25° with respect to the vertical $I|_0(\phi, \varphi) = I_0(\phi)$, that is, independent of the azimuth angle φ . For the finite-aperture sources, calculations were performed for uniform or Gaussian distribution of emitted radiation over the source aperture. According to the data of sodar [14] and lidar measurements [15], the outer scale of turbulence L_0 changes from a few meters to 150 m in the atmospheric boundary layer. In our calculations, it was set equal to 2, 4, 6, 8, 10, 15, 20, 40, 60, and 80m. Acoustic radiation of the source propagated through the plane-parallel layers of the atmosphere with the coefficients of classical and molecular absorption $\sigma_{cl}(i)$ and $\sigma_{mol}(i)$ and scattering on turbulent temperature and wind velocity fluctuations $\sigma_T(i)$ and $\sigma_V(i)$ being constant within these layers, where $i = 1, \dots, 25$. In calculations of their altitude dependence, the vertical profiles of the atmospheric temperature, pressure, and velocity of sound were taken for the standard model of the atmosphere [16].

Figure 1 shows the vertical profiles of the total attenuation coefficient calculated from Eq. (1) for frequencies $F = 1 - 4$ kHz, and Figure 2 shows the vertical profiles of the phonon scattering probability $P_{sc}(i) = [\sigma_T(i) + \sigma_V(i)]/\sigma_{att}(i)$, where σ_T was calculated from Eq. (2) and σ_V was calculated from Eq. (3). It should be noted that at a frequency of 2kHz, the turbulent attenuation becomes comparable with the molecular absorption in the surface layer of the atmosphere for $L_0 \geq 15$ m ($sc(i) \geq 0.5$, see Fig. 2).

As demonstrated in [6], at the frequency $F = 1$ kHz they are comparable for $L_0 \geq 20$ m. In this case, the main contribution to the turbulent attenuation of sound propagating along the vertical direction comes from the dynamic turbulence. The contribution of temperature fluctuations is by 1–2 orders of magnitude

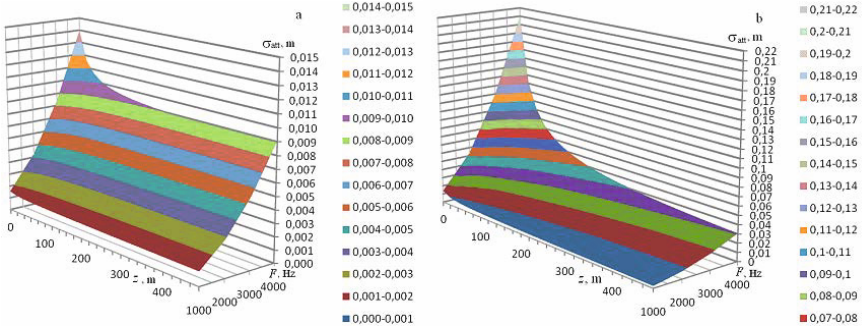


Fig. 1. Vertical profiles of the total attenuation coefficient for $F = 1 - 4$ kHz and $L_0 = 10$ (a) and 80m (b)

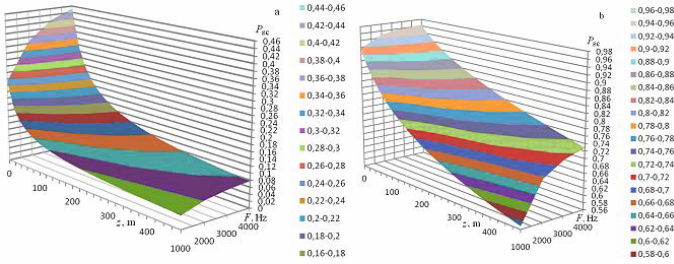


Fig. 2. Vertical profiles of the phonon scattering probability for $F = 1 - 4$ kHz and $L_0 = 10$ (a) and 80m (b)

smaller. This was also pointed out in [4]. From Fig. 1 it can also be seen that in the surface layer, the attenuation coefficient increases approximately by an order of magnitude when the outer scale of turbulence L_0 increases from 10 to 80m. In this case, the phonon scattering probability (Fig. 2) increases from 0.35 to 0.95. These data are confirmed by the results presented in [17], where it was concluded that the magnitude of the excess turbulent attenuation fluctuates in wide limits and can be as great as the classical and molecular absorption.

The normalized phase functions of sound scattering on temperature fluctuations calculated by Eq. (5), and the normalized phase functions of sound scattering on wind velocity fluctuations calculated by Eq. (6) for frequencies in the range 1-4 kHz.

3 Computational Algorithm

To construct a computational algorithm, both standard computational procedures borrowed from [18] and procedures developed in [6, 7, 19] with allowance for the specifics of sound interaction with the atmosphere were used. We considered a point-sized source of acoustic radiation placed at an altitude of 35 m above the ground and having an acoustic power of 1 W. A hypothetical receiver

was placed above the source at an altitude of 500 m from the ground. The coordinates of the point of phonon emission (x_0, y_0, z_0) and their directional cosines $(\omega_1, \omega_2, \omega_3)$ were calculated using the procedure described in [18]. The Earth's surface was considered absolutely absorbing, and when the phonon trajectory intersected the plane $z = 0$, the phonon was considered absorbed, and a new phonon history was modelled. The phonon free path was modelled by the following scheme.

a) Let c be the cosine of the angle between the positive direction of the z axis and the direction of phonon emission; then $\Delta l = dz/c$ be the distance passed by the phonon through atmospheric layers with attenuation coefficients $\sigma_{att}[1], \dots, \sigma_{att}[N]$.

b) By subsequent subtraction, we find the number j of the layer such that

$$\frac{z[1] - z_0}{c} \sigma_{att}[1] + \Delta l \sum_{m=2}^{j-1} \sigma_{att}[m] < \ln(rand) \leq \frac{z[1] - z_0}{c} \sigma_{att}[1] + \Delta l \sum_{m=2}^j \sigma_{att}[m],$$

where $rand$ is a random number uniformly distributed in the interval $[0,1]$.

c) If there is no number j satisfying condition (14), it is considered that the phonon have been escaped from the medium; otherwise,

$$l_{free} = \frac{z[1] - z_0}{c} + \Delta l(j - 2) - \frac{\ln(rand) + \Delta l \sum_{m=2}^{j-1} \sigma_{att}[m]}{\sigma_{att}[j]}.$$

The point of the next collision was chosen by the well-known formulas [18].

Then the collision type was chosen. The following procedure was used.

d) $p_1 = \sigma_{cl}(j)$, $p_2 = \sigma_{mol}(j)$, $p_3 = \sigma_T(j)$, $p_4 = \sigma_V(j)$.

e) $P_1 = p_1$, $P_2 = p_1 + p_2$, $P_3 = p_1 + p_2 + p_3$, $P_4 = p_1 + p_2 + p_3 + p_4$.

f) $F_1 = P_1/P_4$, $F_2 = P_2/P_4$, $F_3 = P_3/P_4$, $F_4 = P_4/P_4 = 1$.

g) $\alpha = rand$, find the number $k = \min\{l : \alpha < F_l\}$.

h) If $k = 1$, classical absorption was simulated; if $k = 2$, molecular absorption; if $k = 3$, scattering on the temperature fluctuations; otherwise, scattering on the wind velocity fluctuations.

In the case of absorption, the phonon was annihilated, and its statistical weight was added to the element of the array determining the value of the acoustic wave intensity absorbed in the j -th atmospheric layer. In the case of scattering, the scattering angle was determined by the scattering phase function given by Eq. (5) for scattering by temperature fluctuations and by Eq. (6) for scattering by wind velocity fluctuations. The procedure of simulation of the scattering angle was described in detail in [20] Calculations were carried out on a personal computer for 10^6 phonon histories, which provided acceptable calculation errors of 3–10%.

4 Calculation Results and Their Discussion

Figure 3 shows dependencies of the transmitted (I_{tr} , W/m^2) and multiply scattered radiation intensities (I_{msc} , W/m^2) over the detector zones for $F = 1.7$ kHz,

$\phi = 5^\circ$ (a and c) and 15° (b and d); $F = 4\text{kHz}$, $\phi = 5^\circ$ (e and g) and 15° (f and h), source altitude $z_s = 35\text{m}$, and outer scale of turbulence, in meters, indicated at the upper right of the figure. Results of our calculations demonstrate that the contribution of multiple scattering I_{msc} to the transmitted radiation intensity I_{tr} within the cone of source radiation increases with the outer scale of turbulence from 10.5% (for $L_0 = 10\text{m}$) to 53% (for $L_0 = 20\text{m}$); for $L_0 = 40\text{m}$, the transmitted radiation intensity is completely determined by multiple scattering. In this case, the sharp decrease of I_{tr} and I_{msc} in Fig. 3 is explained by the fact that received radiation is beyond the limits of the cone of source radiation divergence. Within the cone of source radiation divergence, the multiple scattering contribution increases from $4.7 \cdot 10^{-7}$ to $4.3 \cdot 10^{-6} \text{ W/m}^2$, that is, by 89% when L_0 increases from 10 to 80 m. This increase in multiple scattering contribution virtually compensates for the decrease in the transmitted radiation intensity with increasing outer scale of turbulence and, as can be seen from Fig.3a, the transmitted radiation intensity for $\leq 50\text{m}$ is virtually independent of the outer scale of turbulence.

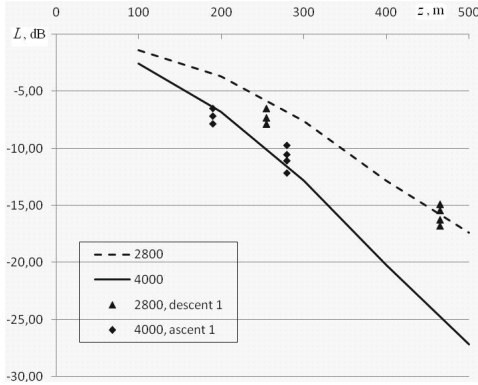


Fig. 4. Total attenuation of acoustic waves propagating along vertical paths versus altitude. Here the solid curves show the results of our Monte Carlo calculations; closed triangles and circles show results of acoustic measurements in [21] with a tethered balloon.

aperture 1 m in diameter and a Gaussian distribution of emitted radiation) with a frequency of 2 kHz demonstrated that in the examined angular source divergence angles, it increased by 66–68% compared to that for the point source. For the uniform distribution of emitted radiation over the source aperture, $I_{tr}(0^\circ, 2.5^\circ)$ remained virtually unchanged. For $F = 3\text{kHz}$, $L_0 = 10\text{m}$, $\phi = 2.5^\circ$, and Gaussian distribution of emitted radiation, $I_{tr}(0^\circ, 2.5^\circ) = 1.6 \cdot 10^{-4} \text{ W/m}^2$, that is, it increased by a factor of 2.2 compared to $I_{tr}(0^\circ, 2.5^\circ) = 7.26 \cdot 10^{-5} \text{ W/m}^2$ for

Figure 4 shows the total attenuation of acoustic waves propagating along vertical paths versus distance. Here the solid curves show the results of our Monte Carlo calculations, and closed triangles and circles show results of acoustic measurements performed in [21] with a tethered balloon. Calculations were performed for the vertical profiles of the atmospheric temperature and relative air humidity measured in [21] during first ascent and descent of the tethered balloon on April 17, 1973. A good agreement of the results of our Monte Carlo calculations with the experimental data [21] can be seen. This demonstrates the efficiency of the developed Monte Carlo algorithm.

Statistical estimates of the transmitted radiation intensity for finite-aperture sources (with a circular

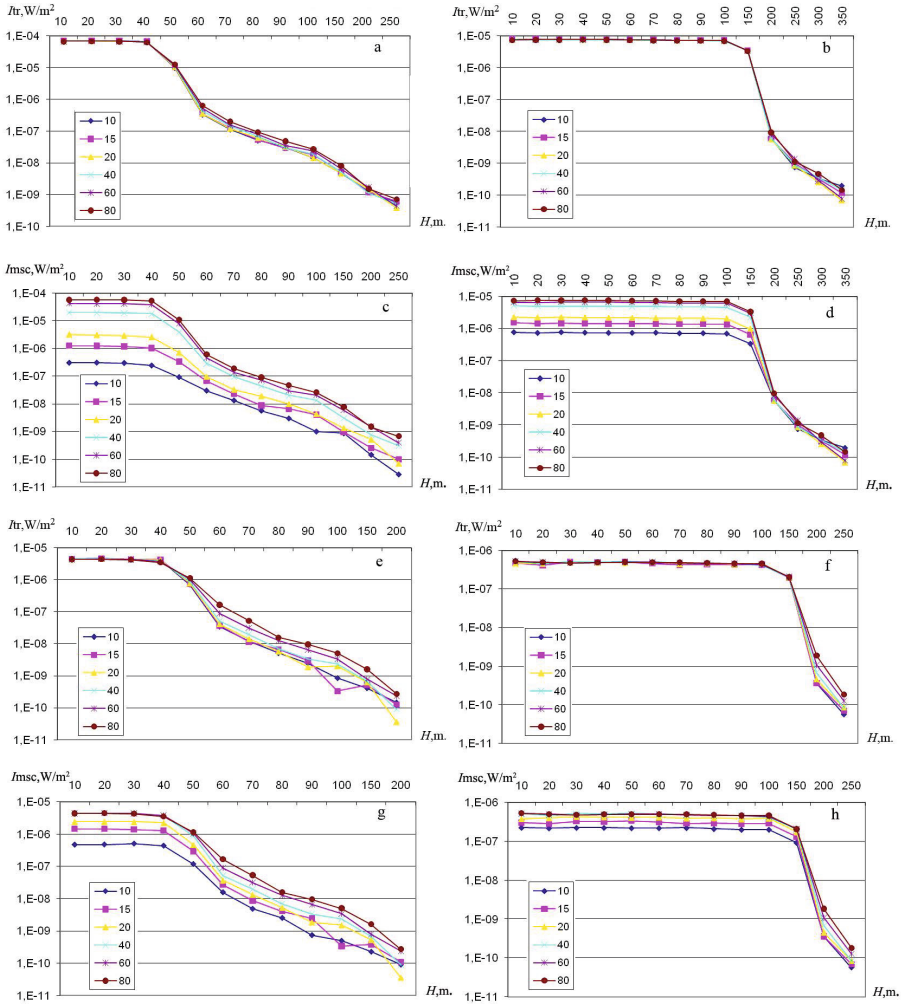


Fig. 3. Distribution of the intensity of transmitted (I_{tr} , W/m^2) and multiply scattered radiation (I_{msc} , W/m^2) over the detector zones for $F = 1.7\text{kHz}$, $\phi = 5$ (a and c) and 15° (b and d); $F = 4\text{kHz}$, $\phi = 5$ (e and g) and 15° (f and h) the indicated values of the outer scale of atmospheric turbulence

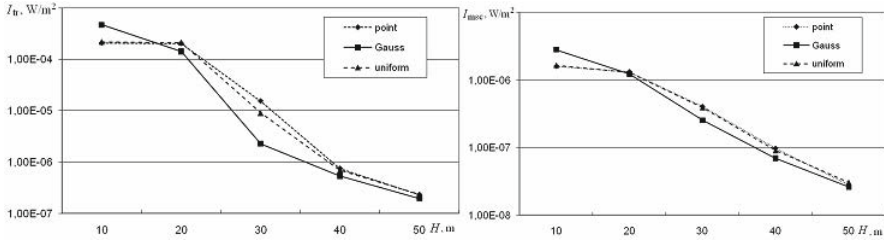


Fig. 5. Effect of the finite circular source aperture ($D = 1\text{m}$) with uniform and Gaussian distributions of emitted radiation on the intensity of transmitted (I_{tr}) and multiply scattered acoustic radiation I_{mcs} for $F = 3\text{kHz}$, $\phi = 2.5^\circ$, and $L_0 = 10\text{m}$

the point source (see Fig. 5). At the same time, it remained virtually unchanged for the uniform distribution of emitted radiation.

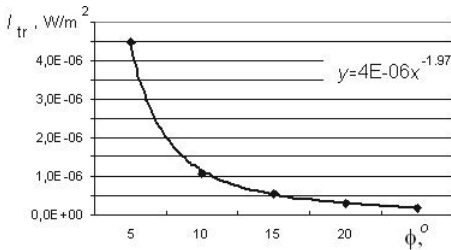


Fig. 6. Dependence of the transmitted radiation intensity on the source divergence angle and its analytical approximation by the power-law dependence (the solid curve) for $F = 4\text{kHz}$ and $L_0 = 10\text{m}$

when the source divergence angle increases from 5 to 25°, I_{tr} decreases by 96%, which is essential and confirms the necessity of application of massive protective shields in sodars [1]. Table 1 below gives values of the corresponding constants A and B entering into formula (17) for $L_0 = 10\text{m}$ and typical sodar frequencies.

Analytical approximation of the results of Monte Carlo calculations by power-law, logarithmic, and exponential dependences demonstrated that they are best described by a power-law dependence of the form

$$I_{tr}(0^\circ, \phi) = A\phi^{-B}, \quad (7)$$

where I_{tr} is in W/m^2 and ϕ is in degrees, with the correlation coefficient close to 1.

Figure 6 shows the dependence $I_{tr}(0^\circ, \phi)$ for the radiation frequency $F = 4\text{kHz}$ and outer scale of turbulence $L_0 = 10\text{m}$. It can be seen that

Table 1. Values of the coefficients in Eq. (7)

F , kHz	A	B
1	$2.8 \cdot 10^{-3}$	2.00
1.7	$1.7 \cdot 10^{-3}$	2.00
2	$1.4 \cdot 10^{-3}$	2.03
3	$2 \cdot 10^{-5}$	2.02
4	$4 \cdot 10^{-6}$	1.97

From Table 1 it follows that the dependence on the source divergence angle is quadratic in character. It is impossible to obtain the dependence of these coefficients on the outer scale of turbulence in this stage, because it is within the limits of the calculation error.

5 Conclusions

Statistical estimates of the contribution of multiply scattered radiation to the intensity of acoustic radiation transmitted through the lower 500-m atmospheric layer demonstrated that for a frequency of 1.7 kHz, it increases from 15 to 80% with the outer scale of atmospheric turbulence. For a frequency of 4.5 kHz, it increases from 30% to the value comparable with the total transmitted radiation intensity.

The contribution of multiple scattering to the transmitted radiation intensity increased with the outer scale of turbulence from 10.5% (for $L_0 = 10\text{m}$) to 53% (for $L_0 = 20\text{m}$); for $L_0 = 40\text{m}$, the transmitted radiation intensity was completely determined by the contribution of multiple scattering. Statistical estimates demonstrate that the intensity of transmitted radiation within the limits of the cone of source radiation is virtually independent of the outer scale of atmospheric turbulence. The decrease in the transmitted radiation intensity with increase in the source divergence angle is quadratic in character. The transmitted radiation intensity I_{tr} decreases by 96% when the source divergence angle increases from 5 to 25°. This is essential and confirms the necessity of application of massive protective shields in sodars. These quantitative estimates can be used for interpretation of results of acoustic sounding and for prediction of the conditions of acoustic radiation propagation in the atmosphere. The results of Monte Carlo calculations are in good agreement with the available experimental data, which confirms the efficiency of the developed Monte Carlo algorithm.

References

1. Krasnenko, N.P.: Acoustic sounding of the atmospheric boundary layer. Publishing House Vodolei, Tomsk (2001)
2. Matuschek, R., Mellert, V., Kephelopoulos, S.: Model calculations with a fast field programme and comparison with selected procedures to calculate road traffic noise propagation under defined meteorological conditions. Acta Acustica United with Acustica 95, 941–949 (2009)
3. Delany, M.E.: Sound propagation in the atmosphere: A historical review. Acustica 38, 201–223 (1977)
4. Razin, A.V.: The mean field method in the problem of acoustic wave propagation in the turbulent atmosphere. Izv. Vyssh. Uchebn. Zaved. Radiofiz 51, 413–424 (2008)
5. Raspet, R., Lee, S.W., Kuester, E., Chang, D.C., Richards, W.F., Gilbert, R., Bong, N.: A fast-field program for sound propagation in a layered atmosphere above an impedance ground. J. Acoust. Soc. Am. 77, 345–352 (1985)
6. Shamanaeva, L.G., Burkatovskaya, Y.B.: Statistical estimates of the multiple scattering contribution to the acoustic radiation intensity transmitted through the lower 500-meter layer of the atmosphere. Russ. Phys. J. (12), 1297–1306 (2004)

7. Shamanaeva, L.G., Burkatovskaya, Y.B.: Statistical estimates of multiple scattering contribution to the transmitted acoustic radiation intensity. In: Proc. 14th Int. Symp. Adv. Bound. Layer Remote Sens, pp. 14–16. Garmish-Partenkirchen (2006)
8. Ostashev, V.E.: Sound propagation in moving media, Nauka, Moscow (1992)
9. Baikalova, R.A., Krekov, G.M., Shamanaeva, L.G.: Statistical estimates of the multiple scattering contribution in sound propagation through the atmosphere. *Opt. Atmos.* 1(5), 25–29 (1988)
10. Tatarskii, V.I.: Wave propagation in the turbulent atmosphere. Nauka, Moscow (1967)
11. ANSI Standard S1–26–1995 (R2009). Method for calculation of the absorption of sound by the atmosphere
12. ISO 9613–1:1996–3–05
13. Shamanaeva, L.G.: The dependence of sound extinction on the parameters of thermal turbulence in the atmospheric boundary layer. *J. Acoust. Soc. Am.* 73(3), 780–784 (1983)
14. Krasnenko, N.P., Shamanaeva, L.G.: Sodar measurements of the structural characteristics of temperature fluctuations and the outer scale of turbulence. *Meteorol. Z.* 7, 392–397 (1998)
15. Banakh, V.A., Rahm, S., Smalikho, I.N., Falits, A.V.: Measurement of atmospheric turbulence parameters by the coherent pulse wind lidar, scanning vertically. *Opt. Atm. Okeana* 20, 1115–1120 (2009)
16. Glagolev, Y.A.: Handbook on the physical parameters of the atmosphere, Gidrometeoizdat, Leningrad (1970)
17. DeLoach, R.: On the excess attenuation of sound in the atmosphere. NASA Technical Note D-7832, Washington (1975)
18. Marchuk, G.I., Mikhailov, G.A., Nazaraliev, M.A., Darbinyan, R.A., Kargin, B.A., Elepov, B.S.: Monte Carlo method in atmospheric optics. Nauka, Novosibirsk (1976)
19. Belov, V.V., Burkatovskaya, Y.B., Krasnenko, N.P., Shamanaeva, L.G.: Statistical estimates of the influence of the angular source divergence angle on the characteristics of transmitted acoustic radiation. *Russ. Phys. J.* (12), 1264–1270 (2009)
20. Krekov, G.M., Shamanaeva, L.G.: Statistical estimates of the spectral brightness of the twilight Earth's atmosphere, pp. 180–186. Atmospheric Optics, Gidrometeoizdat, Leningrad (1974)
21. Aubry, M., Baudin, F., Weil, A., Rainteau, P.: Measurement of the total attenuation of acoustic waves in the turbulent atmosphere. *J. Geophys. Res.* 79(36), 5598–5606 (1974)